Acta of Bioengineering and Biomechanics
Vol. 19, No. 2, 2017

Original paper
DOI: 10.5277/ABB-00783-2016-03

Analysis of the influence of the transducer and its coupling layer on round window stimulation

HOUGUANG LIU[1]*, DAN XU[1], JIANHUA YANG[1], SHANGUO YANG[1], GANG CHENG[1], XINSHENG HUANG[2]

[1] School of Mechatronic Engineering, China University of Mining and Technology, Xuzhou, China.
[2] Department of Otorhinolaryngology-Head and Neck Surgery, Shanghai Zhongshan Hospital affiliated to Fudan University, Shanghai, China.

Purpose: In this work, a finite element study is proposed to evaluate the effects of the transducer and its coupling layer on the performance of round window (RW) stimulation. *Methods*: Based on a set of micro-computer tomography images of a healthy adult's right ear and reverse engineering technique, a coupled finite-element model of the human ear and the transducer was constructed and verified. Then, the effect of the cross-section of the transducer, the elastic modulus of the coupling layer, the mass of the transducer, and the preload of the transducer were studied. *Results*: The increase of the transducer's cross-section area deteriorates the RW stimulation, especially at the lower frequencies. This adverse effect of the cross-section area's increase of the transducer can be reduced by adding a coupling layer between the transducer and the RW. However, the coupling layer's improvement on the RW stimulation is reduced with the increase of its elastic modulus. Moreover, the mass loading of the transducer decreases the RW stimulation's performance mainly at higher frequencies and applying a static preload on the transducer enhances its hearing compensating performance at higher frequencies. *Conclusions*: The influence of the transducer's mass, the mass of the transducer, the applied static preload and the properties of the coupling layer must be taken into account in the design of the RW stimulation type implantable middle ear hearing device.

Key words: *implantable middle ear hearing device, round window stimulation, transducer, coupling layer, finite element analysis*

1. Introduction

Worldwide there is an estimated 500 million people who suffer from hearing loss. Up to now, there is still lack of effective treatment to sensorineural hearing loss. The majority of these patients can only turn to traditional hearing aids. However, traditional hearing aids have several inherent disadvantages, such as sound distortion, limited amplification, noise and ringing, discomfort, and cosmetic appearance [13]. To overcome these limitations, methods alternative to conventional hearing aids have been developed. Implantable middle ear hearing device (IMEHD) is one of these alternative treatments. Over the past decades different types of IMEHDs have been developed [4], [13], [16].

The IMEHD mainly consists of a microphone, a battery, an audio processor, and a transducer. Among them, the transducer is the key component since it provides a direct mechanical stimulation to the human ear's inner components [13]. The ossicular chain is the component that the transducer commonly stimulates, and then the vibration is transmitted into the cochlea through the oval window. However, coupling the transducer to the ossicular chain is difficult for patients with middle ear disease, such as ossicular lesion. To solve this problem, an alternative way of coupling the transducer to the cochlea by driving the round window (RW), called RW stimulation (RW-S), was developed [7], and clinical studies on this novel IMEHD's application have been reported [6], [7], [24].

* Corresponding author: Houguang Liu, School of Mechatronic Engineering, China University of Mining and Technology, Xuzhou 221116, China. Tel: 08618761435299, e-mail: liuhg@cumt.edu.cn

Received: November 10th, 2016
Accepted for publication: January 2nd, 2017

Nonetheless, the clinical results showed that the actual functional gain provided by the RW-S is far less than the theoretic expectancy [6]. To improve the clinical performance of the RW-S, many studies have been carried out. Measuring the stapes velocity and intracochlear sound pressures, Nakajima et al. [20] concluded that the capacity of the RW-S can be boosted by placing a coupling layer, which is a piece of fascia, between the transducer and the RW. Arnold et al.'s experimental results [2] also proved that the sound energy transfer from the RW-S to the cochlea was increased by implanting a subcutaneous connective tissue to underlay the transducer. However, it was not reported which material optimal for the coupling layer of the transducer. Based on a human ear finite element model, Zhang et al. [26] further demonstrated that reducing the transducer's cross-section area can enhance the RW-S' output. Only two sizes (1 mm^2 and 0.314 mm^2, respectively) of the transducer's cross-section area were compared. And both of them are far smaller than current used transducer's value, which is 2.543 mm^2 [7]. Besides, the effect of the coupling layer was not considered in their study.

In addition to the coupling layer and the transducer's cross section, Maier et al. [19] indicated that applied a static preload on the transducer can also improve the efficiency of the RW-S. However, this result is inconsistent with Lupo et al.'s experimental report [18] which stated that the loading pressure change of the transducer did not affect the RW-S' performance. Up to now there is still no theoretical study on this issue.

Considering the tiny and complex structure of the human ear, systematic experimental study on above issues is difficult to conduct. Meanwhile, mechanical model, especially the finite element (FE) model, shows distinct advantages in simulating the complex biological system of the human ear [8], [10] and in aiding the design of IMEHDs [17], [25], [26]. Accordingly, in this paper, to systematically investigate how to improve the clinical output of RW-S, a human ear FE model was constructed via micro-computer tomography imaging and reverse engineering technique. Then, based on this model, study was performed on the influence of four important parameters concerning the design of the RW-S' transducer: the transducer's cross-section area, the elastic modulus of the coupling layer, the transducer's mass and the static preload applied on the transducer. This study results are intended to support the optimization of the transducer in order to improve the RW-S' clinical performance.

2. Materials and methods

2.1. Finite element model of the human ear

Based on a fresh human temporal bone (man, age 45, right ear), a human ear geometric model was obtained by using the micro-computer tomography imaging and the technique of reverse engineering. Then, a FE model of the human middle ear was built by using the FE preprocessing software Hypermesh on the basis of the geometric model. In this FE model, the tympanic membrane (TM) and TM annulus ligament were meshed by 804 there-noded shell elements. The diameter along and perpendicular to manubrium were 9 mm and 7.75 mm, respectively. The thickness of TM annulus ligament, TM pars tensa (PT) and TM pars flaccida (PF) were 0.2 mm [23], 0.05 mm and 0.1 mm [27], respectively. To make the FE model more accurate, a three-layered composite structure of the TM was taken into account [9] and from the inside out the thickness of them were 0.017 mm, 0.016 mm and 0.017 mm, respectively. The ossicles (malleus, incus and stapes) and human middle ear tendons as well as ligaments were meshed by 48043 four-noded tetrahedral elements altogether.

The cochlea was simplified as a fluid-filled straight chamber. This chamber was divided by the basilar membrane (BM) into two similar ducts: scala vestibuli (SV) and scala tympani (ST). These two ducts connected to each other at the apex of the cochlea through a passage called helicotrema. Besides, the cochlea included the OW and the RW – the membrane-covered opening for the SV and ST, respectively. The height and width of the SV and ST were changed linearly from 2 mm, 3.2 mm at the base to 0.4 mm and 0.65 mm at the apex, respectively. The fluid volumes of the SV and ST were 92.315 mm^3 and 93.270 mm^3. Besides, the SV and ST were meshed by tetrahedral elements, and the numbers were 13802 and 17577, respectively. The helicotrema was constructed as a rectangular fluid passageway with a dimension of 0.65 $\times$ 1.6 mm^2. The thickness of RW was set as 0.1 mm [22]. The area of the RW was 2 mm^2, similar to the mean area of 2.08 mm^2 reported by Atturo et al. [3]. According to the observation on histology section in literature [15], a bony wall was constructed and utilized to fully clamp the outer edge of the RW membrane to fix the edge of the RW membrane. The basilar membrane (BM) was meshed into 482 shell elements totally. The thickness and width of the BM changed

linearly from the base to apex: the thickness changed from 7.5 μm to 2.5 μm, and the width changed from 0.15 mm to 0.5 mm.

The impedance produced by human ear canal and middle ear cavity is significantly smaller than that produced by the components of human middle ear and the cochlea [28]. Thus, the ear canal and cavity were not modeled in this paper. The final constructed human ear FE model is shown in Fig. 1.

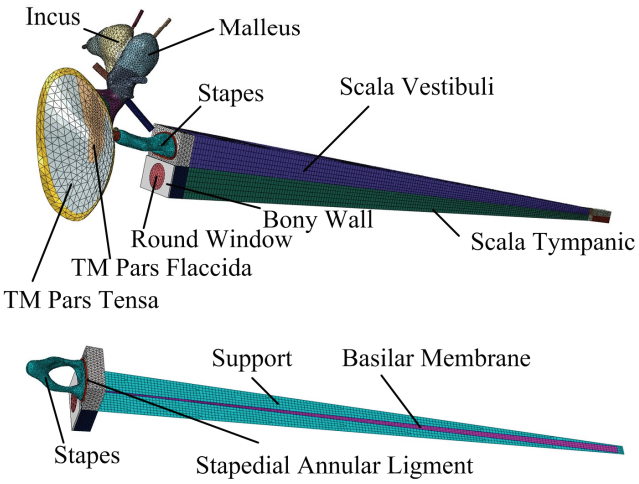

Fig. 1. Finite element model of the human ear

2.2. Material properties

Material properties defined for the human ear were elastic modulus, density and Poisson's ratio. Mechanical properties of the middle ear were defined as homogeneous and isotropic, while the middle layer of the TM PT was orthotropic. Besides, the outer layer and the inner layer of the TM PT were modeled with same elastic properties. Poisson's ratio of each part of human middle ear was all set to 0.3 [8]. The elastic modulus and density of the middle ear's structures initially referred to published reports [8], [9], [22]. Based on literature and cross-calibration of the material parameters of the muscle tendons and ligaments, the final material properties of our human ear model are obtained and listed in Table 1.

The bulk modulus and the density of the cochlea fluid in SV and ST were 2250 MPa and 1000 kg/mm^3 [8], respectively. Considering the stiffness of the BM changing along its length from base to apex, the elastic modulus of the BM was defined as 40 MPa at the base, 15 MPa at the middle and 3 MPa at the apex [22]. The elastic modulus of RW was 0.35 MPa [22], while that of BM support was 14100 MPa [22].

Table 1. Material properties of middle ear components

Component		Elastic modulus (N/m^2)	Density (kg/m^3)
Tympanic annulus ligament		3×10^5 [9]	1.2×10^3 [9]
TM, pars tensa	Layer 1	1×10^7 [9]	1.2×10^3 [9]
	Layer 2	$E_\theta = 2.0 \times 10^7$ [9] $E_r = 3.2 \times 10^7$ [9]	
	Layer 3	1×10^7 [9]	
TM, pars flaccida		1×10^7 [9]	1.2×10^3 [9]
Manubrium		4.7×10^9 [8]	1×10^3 [8]
Malleus handle		1.41×10^{10} [8]	3.7×10^3 [8]
Malleus neck		1.41×10^{10} [8]	4.53×10^3 [8]
Malleus head		1.41×10^{10} [8]	2.55×10^3 [8]
Incus body		1.41×10^{10} [8]	2.36×10^3 [8]
Incus short process		1.41×10^{10} [8]	2.26×10^3 [8]
Incus long process		1.41×10^{10} [8]	5.08×10^3 [8]
Stapes		1.41×10^{10} [8]	2.2×10^3 [8]
Incudomalleoular joint		1.41×10^{10} [8]	3.2×10^3 [8]
Incudostapedial joint		6×10^5 [8]	1.2×10^3 [8]
Lateral mallear ligament		6.7×10^5 [22]	2.5×10^3 [22]
Superior mallear ligament		4.9×10^5 [22]	2.5×10^3 [22]
Anterior mallear ligament		2.1×10^7 [8]	2.5×10^3 [22]
Posterior incudal ligament		6.5×10^7 [22]	2.5×10^3 [22]
Tensor tympani tendon		7×10^7 [8]	2.5×10^3 [22]
Stapedial annular ligament		2×10^5 [8]	1.2×10^3 [22]

Recent experimental study [11], [26] show that human eardrum and some other soft tissues of human ear are viscoelastic. Thus, the viscoelastic material properties were applied to our model's TM PT (inner and outer layers), TM PF, incudostapedial joint (ISJ), incudomallear joint (IMJ), stapedial annular ligament (SAL) and RW. The relaxation modulus of these soft tissues can be expressed as by the equation (1)

$$E(t) = E_0 + E_1 e^{-t/\tau_1} \tag{1}$$

where E_0 was the elastic modulus presented in Table 1, and E_1 and τ_1 were the viscoelastic parameters listed in Table 2 [26]. The energy loss of the rest parts of the human ear were defined as Rayleigh damping: the damping coefficients of middle ear were $\alpha = 0$ s^{-1}, $\beta = 0.75 \times 10^{-4}$ s; those of the BM were $\alpha = 0$ s^{-1}, $\beta = 1 \times 10^{-3}$ s.

Table 2. Viscoelastic material parameters for soft tissues in the ear

	PT	PF	IMJ	ISJ	SAL	RW
E_1 (MPa)	100	16	240	20	10.8	1.0
τ_1 (μs)	25	25	20	20	24	30

2.3. Boundary Conditions

The outer sides of the tendons and ligaments of middle ear, the BM support and the RW were fixed to zero displacement in our human ear FE model. The normal pressure gradient of the cochlea fluid next to the bony wall was set to zero. Besides, fluid structure interfaces were defined at the cochlear fluid elements' surfaces which were connected to movable structures (i.e., the BM, the RW, and the stapes footplate).

2.4. Modeling of the coupling mechanical model

Our main concern was the influence of the transducer's mass and cross-section area on the RW-S, but not the transducer's working mechanism, the inner structure of the transducer was not considered in our modeling process. Therefore, in our established coupling mechanical model of the transducer and the human ear, the transducer and the coupling layer were modeled as solid cylinders using four-node tetrahedral solid elements. One side of the transducer attached to the coupling layer, and the other side of the transducer was driven by an excitation force. The axial length of the transducer was set to 1 mm, considering the length of the SOUNDBRIDGE [7] which is a typical kind of transducer used for RW-S. The cross-section area of the coupling layer remained the same as that of the transducer. The final constructed coupling FE model is shown in Fig. 2.

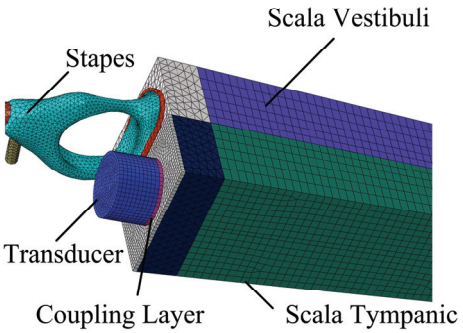

Fig. 2. The coupling FE model of the transducer and the human ear

2.5. Equivalent sound pressure

The BM's movement is responsible for converting the input mechanical vibration into neural signals, which are passed to the brain via the auditory nerve. Thus, the BM's movement is related to human hearing directly. Besides, the BM has frequency selective properties for acoustic signal, which means that the excitation frequency of acoustic signal and the position of peak amplitude on BM are corresponding one by one, and this frequency was called the characteristic frequency of that position. To make RW stimulation's performance equivalent to the one of normal acoustic stimulation, the excited peak amplitudes of the BM displacement for certain frequency should be the same. Thus, the equivalent sound pressure (ESP), which could be calculated using the equation (2), was used to compare the BM displacements induced by the RW stimulation and normal acoustical stimulation at the eardrum, and the ESP was utilized to evaluate the hearing compensating performance of the RW stimulation.

$$P_{\text{eq}} = 100 + 20\log_{10}\left(\frac{d_{\text{rw}}}{d_{\text{ac}}}\right) \tag{2}$$

where d_{ac}, d_{rw} were BM displacements induced by 100 dB SPL eardrum's acoustical stimulation and the RW stimulation, respectively.

3. Numerical results

3.1. Verification of human ear model

The cochlear input impedance is an important parameter reflecting the sound transfer property from the middle ear into the cochlea. It is defined as the ratio of sound pressure produced in the SV at the OW to the volume velocity of fluid at the OW. Fig. 3 shows our model-predicted result compared with experimental reports [1], [21]. The calculated curve is higher than the experimental curves of Aibara et al. [1] between 2000 Hz and 8000 Hz. However, the model-predicted curve has a great agreement with Puria et al's data [21] both in the magnitude and in the trend.

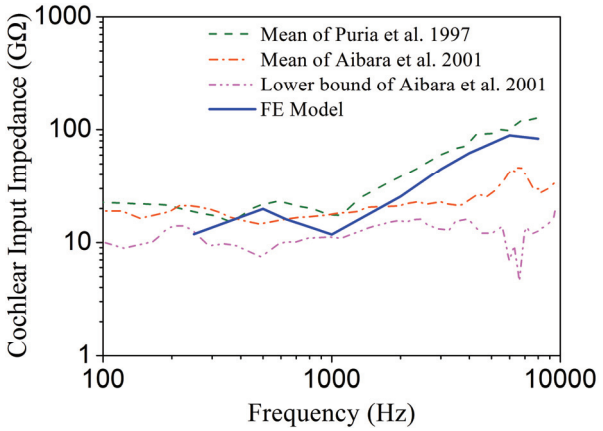

Fig. 3. Cochlear input impedance derived from the FE model compared with published experimental data

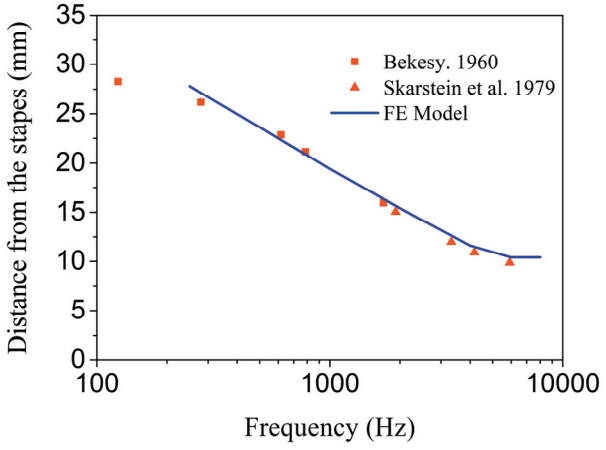

Fig. 4. Position of peak amplitude on the basilar membrane derived from the FE model compared with published experimental data

The frequency selectivity of the BM is a key functional property of the cochlea. Figure 4 shows the comparison of the results got from our FE model with those from the experiments operated by Békésy et al. [5] and Skarstein et al. [14]. It is apparent that the calculated curve lies close to the experimental data: the farther the position away from the stapes on the BM, the smaller the corresponding characteristic frequency. That means that the BM sections closer to the apex are sensitive to the lower-frequency signals while the sections closer to the base are sensitive to the higher-frequency signals, which proved the frequency selectivity of our FE model's BM.

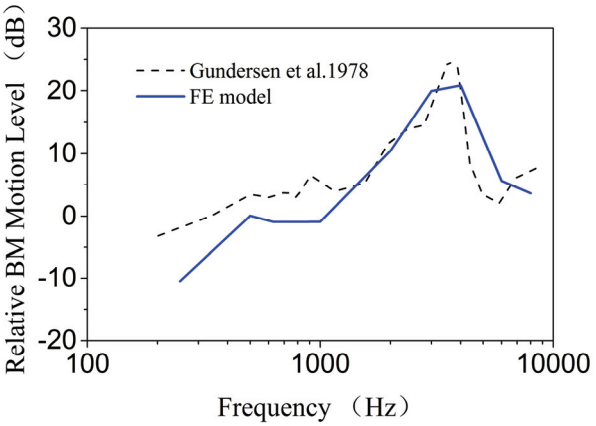

Fig. 5. Level of relative BM velocity at 12 mm from the base derived from the FE model compared with published experimental data

To further verify our FE model, a specific position which is 12 mm away from the base on the BM was taken as a measurement point. The magnitude of the ratio of this specific position's velocity to the stapes footplate's velocity was calculated and compared with Gundersen et al.'s experimental data [12], as shown in Fig. 5. The model-predicted result matches the experimental data well, and the calculated maximum magnitude is 20.83 dB at 4000 Hz. Thus, 4000 Hz is the characteristic frequency of this position which is 12 mm away from the base on the BM, what could also be obtained from Fig. 4.

These comparisons show that our model-predicted results match the experimental results well, which indicates that our FE model could accurately simulate the sound transmission characteristics of the human ear, especially that of the cochlea. Thus, our human ear FE model could be used to study the hearing compensate performance of the RW stimulation.

3.2. Effect of the transducer's cross-section area

The cross-section area is a key design parameter for the transducer. To investigate its influence on the

RW stimulation, the models of the transducers with four different cross-section areas, which were 0.5 mm^2, 1 mm^2, 1.5 mm^2 and 2 mm^2, corresponding to 25%, 50%, 75% and 100% of RW's cross-section area were constructed. And an excitation force of 50 μN was applied on the free side of the transducer to stimulate the BM displacement equivalent to 100 dB SPL at the TM [26].

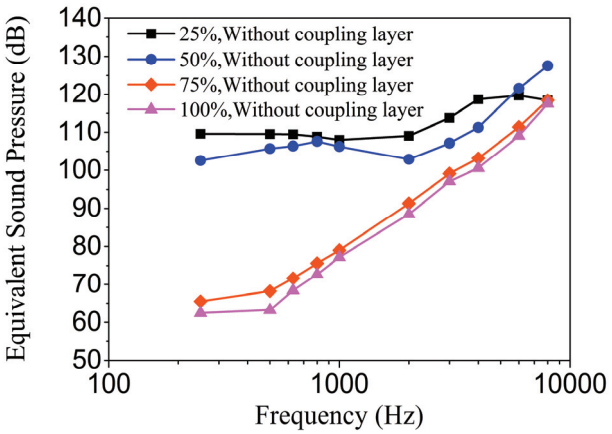

Fig. 6. Effect of the transducer's cross-section area on RW stimulation's ESP without the coupling layer

Figure 6 shows our model-predicted result. It indicates that the increase of the transducer's cross-section area generally reduced the ESP, especially at the lower frequencies (<2000 Hz). The ESP curves with 75% and 100% of the RW area are close to each other. The minimum values of these two curves were 65.4 dB and 62.3 dB at 250 Hz, respectively, while the maximum ones are equal to 118 dB at 8000 Hz. These two curves are lower than the other two ESP curves with 25% and 50% of RW area, especially at the frequencies of 250–2000 Hz; the maximum difference is up to 55 dB at 250 Hz.

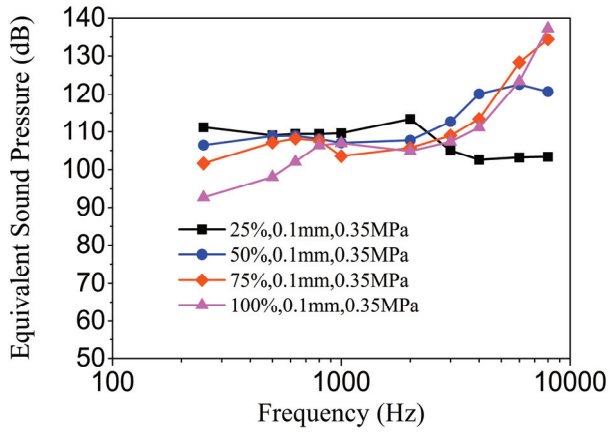

Fig. 7. Effect of the transducer's cross-section area on RW stimulation's ESP with the coupling layer

Considering the current clinical studies always implant a coupling layer between the transducer and the RW, we also incorporated a coupling layer in our model. The coupling layer was built with a thickness of 0.1 mm and a Young's modulus of 0.35 MPa. Figure 7 shows the results calculated by our model. It demonstrates that the introduction of the coupling layer significantly boosted the ESP of the transducers with larger cross-section area (75% and 100% of the RW). The minimum of these two curves were raised to 101.6 dB and 92.8 dB at 250 Hz, respectively, while the maximum ones were all changed to 130.6 dB at 8000 Hz. However, when the transducer's cross-section area is smaller (25% and 50% of the RW), the incorporation of the coupling layer has little impact on RW stimulation's performance. Besides, it also shows that the introduction of the coupling layer diminished the sensitivity of the RW-S' performance to the change of the transducer's cross-section area.

3.3. Effect of coupling layer's elastic modulus

To figure out the influence of the coupling layer's elastic modulus on the RW-S, we changed the coupling layer's elastic modulus from 0.35 MPa to 1.75 MPa, 3.5 MPa, 17.5 MPa and 35 MPa, respectively. These values are corresponding to 1 time, 5 times, 10 times, 50 times and 100 times of the RW's elastic modulus in our model. And the thickness of coupling layer was defined as 0.1 mm, which is similar to the thickness of the round window. Besides, considering the difficulty of small transducer's manufacture, the transducer's cross-section area was set as 2 mm^2, which is equivalent to 100% of the one of the RW. The model-calculated result is shown in Fig.8, which apparently

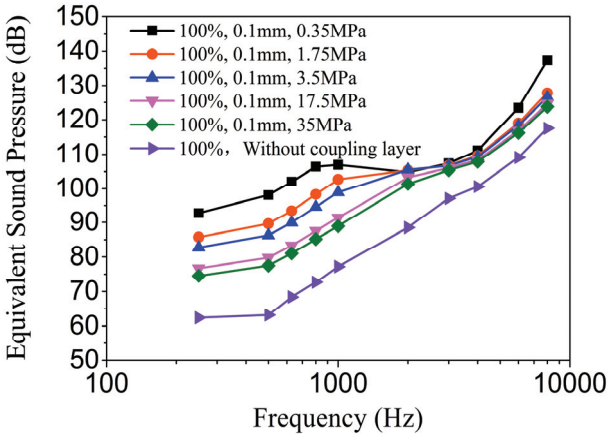

Fig. 8. Effect of the coupling layer's elastic modulus on RW stimulation's ESP

demonstrates that the introduction of the coupling layer did improve the RW stimulation. However, the increase of the elastic modulus of the coupling layer deceased this improvement on the RW stimulation, especially at lower frequencies (<2 kHz).

3.4. Effect of the transducer's mass

Figure 9 shows the model-predicted ESP of different masses of the transducer. In this simulation, the coupling layer's elastic modulus, the coupling layer's thickness and the transducer's cross-section area were set to 0.35 MPa, 0.1 mm and 2 mm^2, respectively. And the mass of the transducer amounted to 2.25 mg, 4.5 mg, 9 mg, 18 mg, 25 mg and 35 mg, respectively. Figure 9 demonstrates that the change of the transducer's mass had little impact on the ESP over the low-middle frequencies of 250–3000 Hz, and the maximum difference of all the ESP curves was only 4.6 dB at 630 Hz. However, the increase of the transducer's mass decreased the ESP severely at higher frequencies (>5 kHz). This allows for the conclusion that the greater the transducer's mass, the greater the decrease of transducer excited ESP in higher frequencies.

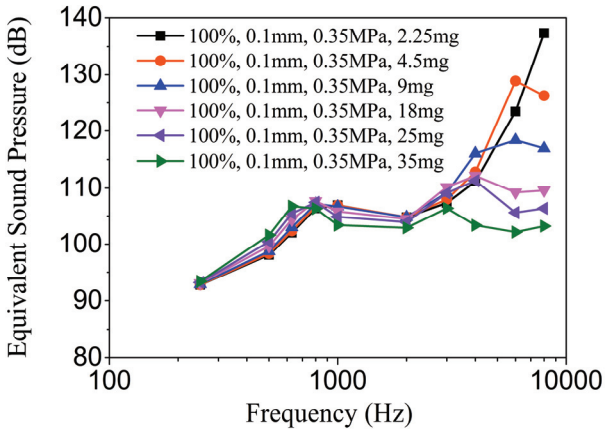

Fig. 9. Effect of the transducer's mass on RW stimulation's ESP

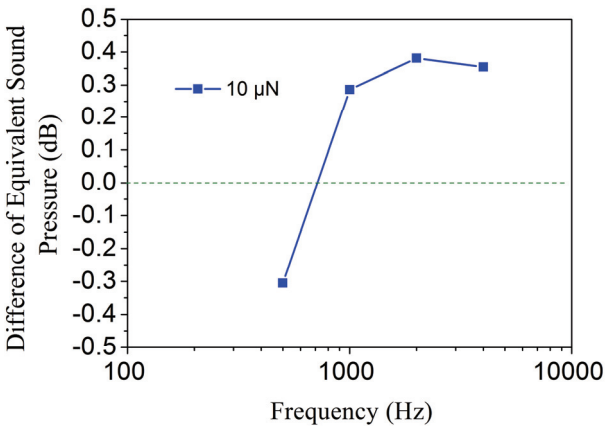

Fig. 10. Effect of the preload on RW stimulation's ESP

3.5. Effect of the static preload applied to the RW

As stated in the introduction section, experimental reports show a discrepancy on the influence of the static preload applied on the transducer. To investigate this influence, a 10 μN-static force on the free side of the transducer was added, apart from its excitation force. This static force is of the same order of magnitude as the transducer's excitation force, which is 50 μN [26]. Figure 10 presents the model-predicted result. It shows that applying a static force on the transducer reduced the RW stimulation slightly in lower frequencies (<700 Hz), but increased it in higher frequencies.

4. Discussion

Cross-section area is one of the main design parameters for the transducer. Zhang et al. found that the RW-S' performance can be increased by reducing its transducer's cross-section area [26]. However, the sizes (1 mm^2 and 0.314 mm^2, respectively) they compared were too smaller than the round window's cross-section area. And they did not consider the size similar to the one of current clinical used transducers, i.e., the SOUNDBRIDGE [7], which has a cross-section area almost equivalent to the one of the RW. Thus, in this work, the transducer's cross-section area was expanded from 0.5 mm^2 to 1 mm^2, 1.5 mm^2 and 2 mm^2, corresponding to 25%, 50%, 75% and 100% of RW's cross-section area, respectively. Our results show the same trend as Zhang et al.'s report [26], that is, the transducer's cross-section area's decrease enhanced RW-S' performance, especially at lower frequencies (below 2000 Hz). In addition, we found that this trend become significant when the transducer's cross-section area is larger than 75% of RW's cross-section area. This is mainly because when the transducer has a diameter similar to the one of the round window, the transducer's motion to the round window can be hindered by the bony structure surrounding the round window. Therefore, in the

design of the RW-S' transducer, its cross-section area should be restricted.

Unfortunately, because of the capacity of the manufacturing process, it is difficult to decrease the transducer's cross-section area, such as the transducer that was used currently. In this case, the results suggest introducing a coupling layer between the transducer and the RW, as this can increase the transducer's performance prominently when the transducer has a larger cross-section area. This conforms to Nakajima et al. [20] and Arnold et al.'s [2] temporal bone experimental results. Besides, a coupling layer material with an elastic modulus similar to the one of the round window membrane is optimal for this transducer. This may occur because the softer coupling layer is easy to deform for transmitting the transducer's motion to the round window membrane. Whereas, it is interest to find out that the incorporation of the coupling layer influenced the transducer's performance slightly and even diminished it at higher frequencies when the transducer's cross-section area was small. Thus, in term of the transducer's performance's enhancement, a coupling layer is required when the transducer's cross-section area is large, and the coupling layer can be omitted when the transducer has a small cross-section area.

The enlargement of the transducer's mass deteriorated the transducer's performance at higher frequencies, but increased it slightly at lower frequencies. This may be caused by to the fact that the increased mass of the transducer changed the system's resonance to lower frequencies. Considering that most sensorineural hearing loss is severe in the high frequencies, this side effect of the transducer's mass loading is extremely detrimental to the performance of RW-S. Therefore, the transducer's mass should be restricted in the design of the RW-S' IMEHD.

In term of the static preload applied on the transducer, Lupo et al. [18] concluded that it has no effect on RW-S' performance, which is discrepancy with Maier et al.'s [19] results. Our results demonstrate that the static preload can reduce the RW-S slightly in lower frequencies, but increase it in higher frequencies. But the influence of the static force is small and difficult to be detected in experiment, which may be the reason why Lupo et al. [18] reported that the loading pressure change of the transducer did not affect the RW-S' performance. Likewise, considering that the most sensorineural hearing loss is severe in the high frequencies, it is beneficial to apply a static preload on the transducer to enhance its hearing compensating performance.

5. Conclusions

A human ear coupling FE model consisting of a RW driving transducer and a coupling layer was constructed via micro-computer tomography imaging and the technique of reverse engineering. The validity of the model was verified by comparing the model calculated results with experimental data. Based on this model, the influence of transducer and its coupling layer on the RW stimulation was studied. The results show:

(1) The increase of the transducer's cross-section area deteriorates the RW stimulation, especially at the lower frequencies. This adverse effect of the cross-section area's increase of the transducer can be reduced by adding a coupling layer between the transducer and the RW. However, the coupling layer's improvement on the RW stimulation is reduced with the increase of its elastic modulus.
(2) The mass loading of the transducer deteriorates RW stimulation's performance prominently in higher frequencies: the greater the transducer's mass the greater the decrease of transducer excited ESP in higher frequencies.
(3) Applying a static preload on the transducer decreases the RW stimulation's performance slightly at lower frequencies but boosts that at higher frequencies. Considering that most sensorineural hearing loss is severe in the high frequencies, implanting a transducer with a preload is preferred.

Acknowledgements

This work was supported by National Natural Science Foundation of China (No. 51305442), the Jiangsu Provincial Natural Science Foundation (No. BK20130194), the Top-notch Academic Programs Project of Jiangsu Higher Education Institutions, and the Priority Academic Program Development of Jiangsu Higher Education Institutions.

References

[1] AIBARA R., WELSH J.T., PURIA S., GOODE R.L., *Human middle-ear sound transfer function and cochlear input impedance*, Hearing. Res., 2001, 152(1–2), 100–109.
[2] ARNOLD A., STIEGER C., CANDREIA C., PFIFFNER F., KOMPIS M., *Factors improving the vibration transfer of the floating mass transducer at the round window*, Otol. Neurotol., 2010, 31(1), 122–128.
[3] ATTURO F., BARBARA M., RASK-ANDERSEN H., *Is the human round window really round? An anatomic study with surgical implications*, Otol. Neurotol., 2014, 35(8), 1354–1360.

[4] BALL G.R., *The vibrant soundbridge: Design and development*, Adv. Oto-Rhino-Laryng., 2010, 69, 1–13.
[5] BÉKÉSY G.V., *Experiments in hearing*, McGraw-Hill, 1960.
[6] BELTRAME A.M., MARTINI A.S., GIARBINI N., STREITBERGER C., *Coupling the Vibrant Soundbridge to cochlea round window: auditory results in patients with mixed hearing loss*, Otol. Neurotol., 2009, 30(2), 194–201.
[7] COLLETTI V., SOLI S.D., CARNER M., COLLETTI L., *Treatment of mixed hearing losses via implantation of a vibratory transducer on the round window*, Int. J. Audiol., 2006, 45(10), 600–608.
[8] GAN R.Z., REEVES B.P., WANG X., *Modeling of sound transmission from ear canal to cochlea*, Ann. Biomed. Eng., 2007, 35(12), 2180–2195.
[9] GENTIL F., PARENTE M., MARTINS P., GARBE C., JORGE R.N., FERREIRA A., TAVARES J.M.R.S., *The influence of the mechanical behaviour of the middle ear ligaments: A finite element analysis*, P. I. Mech. Eng. H., 2011, 225(1), 68–76.
[10] GENTIL F., PARENTE M., MARTINS P., SANTOS C., ALMEIDA E., FERREIRA A., NATAL R., *Numerical study of Hough technique in surgery of otosclerosis, using the finite element method*, Acta. Bioeng. Biomech., 2015, 17(4), 149–153.
[11] GHADARGHADAR N., AGRAWAL S.K., SAMANI A., LADAK H.M., *Estimation of the quasi-static Young's modulus of the eardrum using a pressurization technique*, Comput. Meth. Prog. Bio., 2013, 110(3), 231–239.
[12] GUNDERSEN T., SKARSTEIN O., SIKKELAND T., *A study of the vibration of the basilar membrane in human temporal bone preparations by the use of the Mossbauer effect*, Acta. Otolaryngol., 1978, 86(3–4), 225–232.
[13] HONG E.P., KIM M.K., PARK I.Y., LEE S.H., ROW Y., CHO J.H., *Vibration Modeling and design of piezoelectric floating mass transducer for Implantable middle ear hearing devices*, Ieice. T. Fund. Electr., 2007, E90a(8), 1620–1627.
[14] KRINGLEBOTN M., GUNDERSEN T., KROKSTAD A., SKARSTEIN O., *Noise-induced hearing losses. Can they be explained by basilar membrane movement?*, Acta. Oto-Laryngologica., 1979, 360, 98–101.
[15] LI P.M., WANG H., NORTHROP C., MERCHANT S.N., NADOL J.B., *Anatomy of the round window and hook region of the cochlea with implications for cochlear implantation and other endocochlear surgical procedures*, Otol. Neurotol., 2007, 28(5), 641–648.
[16] LIU H.G., TA N., MING X.F., RAO Z.S., *Design of floating mass type piezoelectric actuator for implantable middle ear hearing devices*, Chin. J. Mech. Eng., 2009, 22(2), 221–226.
[17] LIU H., GE S., CHENG G., YANG J., RAO Z., HUANG X., *The effect of implantable transducers on middle ear transfer function – a comparative numerical analysis*, J. Mech. Med. Biol., 2016, 16(04), 1650040.
[18] LUPO J.E., KOKA K., HYDE B.J., JENKINS H.A., TOLLIN D.J., *Physiological assessment of active middle ear implant coupling to the round window in Chinchilla lanigera*, Otolaryng. Head. Neck., 2011, 145(4), 641–647.
[19] MAIER H., SALCHER R., SCHWAB B., LENARZ T., *The effect of static force on round window stimulation with the direct acoustic cochlea stimulator*, Hearing. Res., 2013, 301(7), 115–124.
[20] NAKAJIMA H.H., DONG W., OLSON E.S., ROSOWSKI J.J., RAVICZ M.E., MERCHANT S.N., *Evaluation of round window stimulation using the floating mass transducer by intracochlear sound pressure measurements in human temporal bones*, Otol. Neurotol., 2010, 31(3), 506–511.
[21] PURIA S., PEAKE W.T., ROSOWSKI J.J., *Sound-pressure measurements in the cochlear vestibule of human-cadaver ears*, J. Acoust. Soc. Am., 1997, 101(1), 2754–2770.
[22] TIAN J.B., HUANG X.S., RAO Z.S., TA N., XU L.F., *Finite element analysis of the effect of actuator coupling conditions on round window stimulation*, J. Mech. Med. Biol., 2015, 15(4), 1550048.
[23] VOLANDRI G., PUCCIO P.D., FORTE P.,CARMIGNANI C., *Biomechanics of the tympanic membrane*, J. Biomech., 2011, 44(7), 1219–1236.
[24] ZERNOTTI M.E., ARAUZ S.L., DI GREGORIO M.F., ARAUZ S.A., TABERNERO P., ROMERO M.C., *Vibrant Soundbridge in congenital osseous atresia: multicenter study of 12 patients with osseous atresia*, Acta. Otolaryngol., 2013, 133(6), 569–573.
[25] ZHANG J., TIAN J., TA N., HUANG X., RAO Z., *Numerical evaluation of implantable hearing devices using a finite element model of human ear considering viscoelastic properties*, P. I. Mech. Eng. H., 2016, 230(8), 784–794.
[26] ZHANG X., GAN R.Z., *A comprehensive model of human ear for analysis of implantable hearing devices*, IEEE. T. Biomed. Eng., 2011, 58(10), 3024–3027.
[27] ZHANG X.M., GUAN X.Y., NAKMALI D., PALAN V., PINEDA M., GAN R.Z., *Experimental and modeling study of human tympanic membrane motion in the presence of middle ear liquid*, J. Assoc. Res. Oto., 2014, 15(6), 867–881.
[28] ZWISLOCKI J., *Analysis of the middle-war function*. Part I: *Input impedance*, J. Acoust. Soc. Am., 1962, 34(9B), 1514–1523.